

**Magnetoresistance and its relation to magnetization in Ni<sub>50</sub>Mn<sub>35</sub>Sn<sub>15</sub> shape-memory epitaxial films**

J. Dubowik, K. Zaski, I. Gociaska, H. Gowiski, and A. Ehresmann

Citation: [Applied Physics Letters](#) **100**, 162403 (2012); doi: 10.1063/1.4704562

View online: <http://dx.doi.org/10.1063/1.4704562>

View Table of Contents: <http://scitation.aip.org/content/aip/journal/apl/100/16?ver=pdfcov>

Published by the [AIP Publishing](#)

---

**Advertisement:**



**Goodfellow**

metals • ceramics • polymers  
composites • compounds • glasses

**Save 5% • Buy online**  
70,000 products • Fast shipping

# Magnetoresistance and its relation to magnetization in $\text{Ni}_{50}\text{Mn}_{35}\text{Sn}_{15}$ shape-memory epitaxial films

J. Dubowik,<sup>1,(a)</sup> K. Załęski,<sup>1</sup> I. Gościańska,<sup>2</sup> H. Głowiński,<sup>1</sup> and A. Ehresmann<sup>3</sup>

<sup>1</sup>*Institute of Molecular Physics, Polish Academy of Sciences, M. Smoluchowskiego 17, PL-60179 Poznań, Poland*

<sup>2</sup>*Department of Physics, A. Mickiewicz University, Umultowska 85, PL-61614 Poznań, Poland*

<sup>3</sup>*Department of Physics and Center for Interdisciplinary Nanostructure Science and Technology (CINaT), University of Kassel, Heinrich-Plett-Str. 40, D-34132 Kassel, Germany*

(Received 20 February 2012; accepted 31 March 2012; published online 17 April 2012)

The magnetoresistance (MR) of Heusler alloy  $\text{Ni}_{50}\text{Mn}_{35}\text{Sn}_{15}$  epitaxial films on MgO substrates is studied as a function of temperature  $T$  and magnetic field  $H$ . The large negative MR extends over martensitic transformation with maximum of  $-22\%$  at 110 K. In martensitic and austenitic phase, the MR is  $-3\%$  and  $-5\%$ , respectively. We show that the MR is governed mainly by magnetization paraprocess at high magnetic fields and scales as the square of magnetization  $\Delta m(H, T)^2$ . © 2012 American Institute of Physics. [<http://dx.doi.org/10.1063/1.4704562>]

A large magnetoresistance (MR) observed in some magnetic shape-memory Heusler alloys (HA) has been generating much interest. Magnetic shape-memory properties occur in HA, which undergo a martensitic transformation (MT) from a cubic austenitic phase (AP) to a martensitic phase (MP) of a lower symmetry. In response to an applied magnetic field, these alloys show a large change in shape.<sup>1</sup> In off-stoichiometric Ni-Mn-X (X = Sn, Sb, In) HA, the shape change is caused by magnetic field induced structural martensitic transformation.<sup>2</sup> In opposite to Ni-Mn-Ga HA, magnetism in Ni-Mn-X is involved in their functional properties through the Zeeman energy (ZE) difference between MP and AP.<sup>3</sup> It leads to magnetic field induced reverse phase transformation (MFIRPT) (Ref. 4) and controls their functional properties such as the large negative MR (Ref. 4) and inverse magnetocaloric effect.<sup>5</sup> In particular, MR in Ni-Mn-X may be as high as  $\approx 60\%$ ,<sup>6</sup> while it is of 5%–8% in Ni-Mn-Ga.<sup>7</sup> The highest values of MR are always at MT. Far from MT, the MR is of a few % in AP and MP.<sup>3,4</sup> Therefore, the large MR is solely attributed to MFIRPT (Ref. 4) or magnetostructural transformation.<sup>3</sup> Singh and Biswas<sup>3</sup> have argued that the origin of less MR below and above MT can be understood through the experimental data fitting with a functional relationship  $\text{MR} = \alpha(\mu_0 H)^n$ , where  $\alpha$  is the strength of the MR and  $0.5 \leq n < 2$  determines the shape of isothermal  $\text{MR}(H)$ . They have linked the changes in  $n$  with various scattering mechanisms. Whatever the precise microscopic model, it is expected that the MR can be captured by a simple scaling form of magnetization as defined by the earlier theories of spin disorder scattering in ferromagnetic (FM)<sup>8</sup> and in antiferromagnetic (AFM) materials.<sup>9</sup> Here, we show that the MR can be consistently explained in the framework of a phenomenological approach involving magnetization changes, which are connected with the presence of AFM interactions.

$\text{Ni}_{50}\text{Mn}_{35}\text{Sn}_{15}(001)$  films 200–400 nm (Ni-Mn-Sn hereafter) in thickness were deposited on MgO(001) substrates

by sputtering at 350 °C in a 2 mTorr Ar pressure.<sup>10</sup> Then, the films were annealed *in situ* at 800 °C for structural ordering. X-ray diffraction (Co-K $\alpha$ ) was used to establish structural ordering.<sup>10</sup> X-ray fluorescence analysis was used to determine composition of the films. Samples composition  $\text{Ni}_{50}\text{Mn}_{35}\text{Sn}_{15}$  was established using several cross-checks with reference samples of stoichiometric films. The actual composition is determined with the accuracy of 1%. The x-ray  $\Theta-2\Theta$  scan shown in the inset of Fig. 1 reveals Ni-Mn-Sn(001) orientation on MgO(001). The full width at half maximum of Ni-Mn-Sn peaks are about 0.5° for (200) and (400) reflections what confirms that the chemically ordered structure has been achieved. Lattice parameter is of 0.598 nm and fits well  $\sqrt{2}a_{\text{MgO}} = 0.595$  nm. Since Ni-Mn-Sn films have been annealed at 800 °C and the thermal

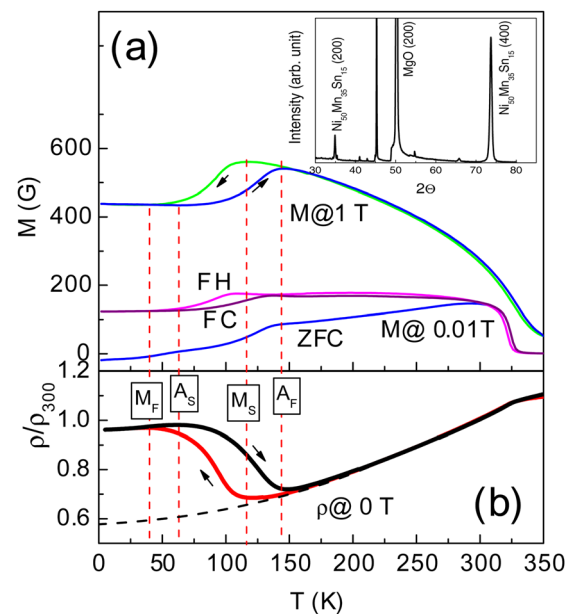


FIG. 1. (a)  $M(T)$  of  $\text{Ni}_{50}\text{Mn}_{35}\text{Sn}_{15}$  film (ZFC, FC, FH) at 0.01 T (bottom plots) and at 1 T (upper plots). (b) Temperature dependence of resistivity  $\rho(T)$  at 0 T on cooling and heating. Thick dashed curve depicts  $\rho(T)$  of  $\text{Ni}_{50}\text{Mn}_{25}\text{Sn}_{25}$  film. Inset shows room temperature XRD of  $\text{Ni}_{50}\text{Mn}_{35}\text{Sn}_{15}$  epitaxial film.

<sup>a)</sup> Author to whom correspondence should be addressed. Electronic mail: [dubowik@ifmpan.poznan.pl](mailto:dubowik@ifmpan.poznan.pl).

expansion of MgO ( $8 \times 10^{-6} \text{ K}^{-1}$ ) is lower than that of HA ( $15 \times 10^{-6} \text{ K}^{-1}$  for  $\text{Ni}_2\text{MnGa}$ ),<sup>11</sup> we expect that the epitaxial Ni-Mn-Sn films are at in-plane tensile strain and MT takes place under constraint.<sup>12</sup> Magnetization and magnetotransport measurements were performed in a commercial Physical Property Measurement System (PPMS) from 4 K to 350 K in a magnetic field up to 9 T applied perpendicular to plane.

A splitting between zero-field-cooled (ZFC), field-cooled (FC), and field-heated (FH) termomagnetization  $M(T)$  at 0.01 T [Fig. 1(a)—three plots at the bottom] implies the presence of magnetically inhomogeneous phase with AFM interactions extended to AP.<sup>5</sup> The difference between FC and FH around MT is due to thermal hysteresis in the first-order transition with a characteristic sequence [Fig. 1(b)] of martensite/austenite (M/A) start/finish (S/F)  $M_S, M_F, A_S,$  and  $A_F$  transformation temperature, respectively. In comparison with the hysteresis of bulk alloys,<sup>3,4</sup> it is much broadened (of 80 K), which may be accounted for by both a small composition gradient and a tensile strain.<sup>12</sup> The upper plots in Fig. 1(a) show temperature dependence of magnetization  $M(T)$  measured at 1 T. The most relevant feature is that the magnetization in MP is much lower than that in AP with  $\Delta M \approx -30\%$ . The decrease in  $M$  is due to closer Mn-Mn positions, which become AFM coupled.<sup>4,5,13,14</sup>

Resistivity  $\rho(T)$  [Fig. 1(b)] changes with temperature in a way closely corresponding to that of magnetization. Important is that  $\Delta\rho_{MA} = (\rho_M - \rho_A)/\rho_A$  ( $\rho_M$  and  $\rho_A$  are the resistivities at MT for the martensitic and austenitic phases, respectively) is of about 50%–60% and does not depend on  $H$  except some substantial shift to lower temperatures (not shown). Resistivity increases rather as a combined effect of AFM spin-correlations below MT and disorder than due to scattering from various orientations of martensitic variants.<sup>15</sup> The presence of the AFM correlations is important in transport and magnetotransport in Ni-Mn-X HA. For Ni-Mn-Ga alloys, MT undergoes in FM phase with  $\Delta M \approx +1 - 10\%$ <sup>16</sup> and the respective  $\Delta\rho_{MA}$  is of about 1%–10%.<sup>7</sup> For nonmagnetic NiTi shape-memory alloy,  $\Delta\rho_{MA} \approx 10\%$  at most.<sup>17</sup> In contrast, for Ni-Mn-X with AFM interactions  $\Delta\rho_{MA}$  may be as large as 100% for Ni-Mn-Sn (Ref. 14) or even 200% for  $\text{Ni}_{50}\text{Mn}_{34}\text{In}_{16}$ .<sup>6</sup> Hence, a jump in resistivity is substantially higher in N-Mn-X HA with AFM correlations than in other shape-memory alloys with no AFM interactions.

Figure 2 shows magnetoresistance  $\text{MR} = [\rho(H, T) - \rho(0, T)]/\rho(0, T)$  typical of our epitaxial Ni-Mn-Sn films as a

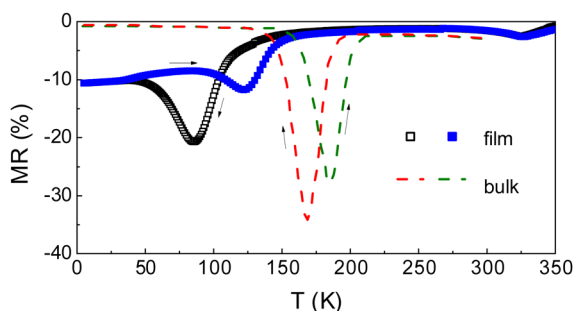


FIG. 2. MR as a function of temperature at 5 T for  $\text{Ni}_{50}\text{Mn}_{35}\text{Sn}_{15}$  film (open symbols) and for  $\text{Ni}_{50}\text{Mn}_{35}\text{Sn}_{15}$  alloy (Ref. 3) (dashed curves).

function of  $T$  at  $\mu_0 H = 5 \text{ T}$  in comparison with that measured for a bulk  $\text{Ni}_{50}\text{Mn}_{35}\text{Sn}_{15}$  (Ref. 3) at the same field (dashed curves). The  $-22\%$  MR at 80 K (on cooling) is somewhat smaller than  $-36\%$  MR for the bulk sample at 170 K. The hysteretic behavior and the characteristic asymmetry are the same as in bulk alloys<sup>3</sup> except the width of hysteresis due to a high tensile strain in epitaxial films.<sup>12</sup> The large MR values in MP for the film sample result from the fact that  $\text{MR}(T)$  was evaluated from resistivity versus temperature courses  $\rho(0 \text{ T}, T)$  and  $\rho(5 \text{ T}, T)$  [not shown in Fig. 1(b)]. We will show later that such a procedure does not include irreversible changes of a AFM to FM phase ratio in MP, i.e., a kinetic arrest.<sup>6</sup> Therefore, we will further discuss the MR measured in isothermal conditions.

Following the line of reasoning by Singh and Biswas,<sup>3</sup> we show in Fig. 3(a) the field dependencies of MR taken at various temperatures with the following procedure. Before measurement, the film was first heated above 350 K and cooled down (ZFC) to 4 K. After heating to the required temperature, MR was measured on cycling the field from 0 T to  $\pm 9 \text{ T}$  and back to 0 T. It is seen that MR both in MP and AP “almost” linearly depends on  $H$ . At  $H = 9 \text{ T}$ , the MR is  $-3\%$  and  $-4.5\%$  at 30 K and 170 K, respectively. In the vicinity of MT, the  $\text{MR}(H)$  increases up to 20% (1—the first course from 0 T to 9 T) and after the kinetic arrest<sup>6</sup> it attains a characteristic concave and convex behavior for the courses (2, 4) and (3), respectively. In Fig. 3(b), we show the respective magnetization  $M(H)$  as a function of magnetic field measured in the same conditions. It is seen that in MT region  $M(H)$  is also highly irreversible with respect to the magnetic field and well corresponds to that of  $\text{MR}(H)$ . In MP and AP, the magnetization is almost reversible but it shows no signature of saturation characteristic to a paraprocess even in AP.

Figure 4 shows the main characteristics of  $\text{MR}(T)$  measured in the isothermal conditions in more details. In Fig. 4(a),  $\text{MR}(T)$  is shown for the first cycle (I) and for the further cycles (II) as it is explained in the inset. It is seen that at 100 K MR attains  $-22\%$  for the first cycle. For the other cycles it is only about  $-10\%$  since we estimate that  $\sim 40\%$  of the sample has transformed to the arrested austenitic phase. Presumably, a mixed magnetic state of the constrained film changes in that way that some of AP is energetically preferable at and below MT. Figure 4(b) shows temperature dependence of parameter  $n$  determined from the

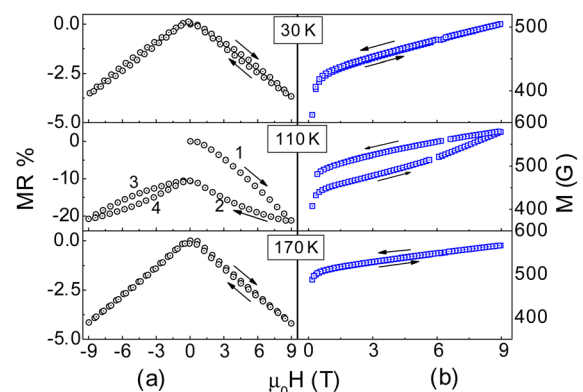


FIG. 3. Isothermal MR (a) and  $M(T)$  (b) measured in MP (30 K), in MT region (110 K), and in AP (170 K).

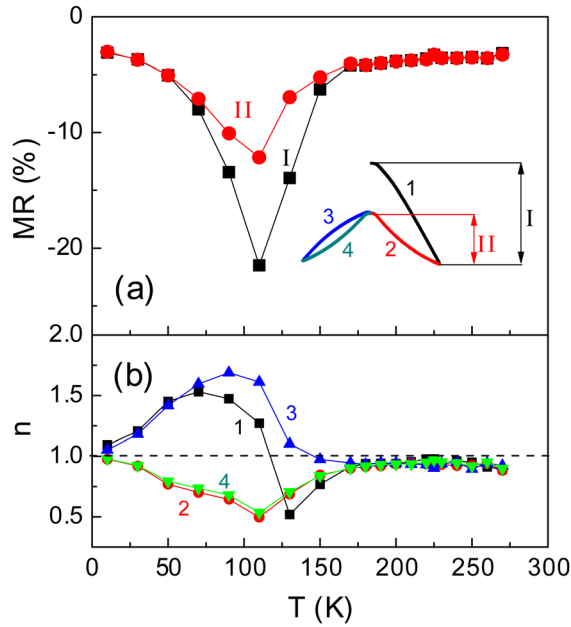


FIG. 4. (a) Maximal MR as a function of temperature determined from isothermal MR measurements in four field scans shown in inset. (b) Temperature dependence of parameter  $n$  obtained from fitting of experimental data to  $\alpha(\mu_0 H)^n$ .

$\alpha(\mu_0 H)^n$  fits to the isothermal MR( $H$ ) for each field cycle. Though the parameter  $n$  is merely related to the shape of MR( $H$ ), it may give a clue on the influence of  $H$  on irreversible and reversible changes in magnetic microstructure as the field is sweeping. For the first cycle, in the vicinity of MT there are irreversible changes in  $n$ , which strongly depend on  $T$ . At MT,  $n$  increases from 0.5 (at 125 K) to  $\approx 1.5$  at 90 K. For the further cycles,  $n$  changes with  $T$  in a monotonic way since the microstructure is already settled. Far from MT,  $n \approx 1$  both in MP and AP.

In opposite to former interpretation of MR in Ni-Mn-X (Ref. 3) and Ni-Mn-Ga,<sup>18</sup> we explain magnetotransport in Ni-Mn-Sn in terms of a simple phenomenological model. The model consists in that the main features of MR can be described by a simple scaling form resulting from spin fluctuations even far from transformation temperature.<sup>8</sup> Therefore, the magnetization fluctuations give rise to magnetoresistance. Below the phase transitions, fluctuations freeze out and relaxation time of scattering increases sharply causing less or more pronounced kink in the resistivity of a ferromagnet at  $T_C$  (Ref. 8) [see Fig. 1(b)] or resistivity maximum for an antiferromagnet below the Neel temperature  $T_N$ .<sup>9</sup> In the simplest case,<sup>8</sup> the temperature (and field) dependence of resistivity of a ferromagnet can be regarded as governed by its magnetic part  $\propto [1 - m(H, T)^2]$ , where  $m(H, T) = M(H, T)/M_{S_0}$ .  $M_{S_0}$  is the saturation magnetization at  $T=0$ . Accordingly, the magnetoresistance of a ferromagnet can be expressed as

$$\text{MR} \propto \frac{m(H, T)^2 - m(0, T)^2}{1 - m(0, T)^2} \propto m(H, T)^2 - m(0, T)^2. \quad (1)$$

Since  $1 - m(0, T)^2$  has a meaning of a scaling factor at a given temperature, we drop it for simplicity. Essential is that we replace the functional relation<sup>3</sup> with the phenomenologi-

cal model, which originates from spin disorder scattering.<sup>8</sup> A similar situation occurs for a pure FM-AFM first order transformation.<sup>19</sup> For FM-AFM transformation, the resistivity is also governed by spin disorder scattering.<sup>9</sup> Similarly to the resistivity in ferromagnets, a magnetic part of resistivity for antiferromagnets  $\rho_{\text{AFM}}$  is proportional to  $1 - m_Q(H, T)^2 / [1 - \Gamma m_Q(H, T)]$ , where  $m_Q(H, T)$  is normalized staggered magnetization with antiferromagnetic wave-vector  $Q$ .<sup>9</sup> The coefficient  $\Gamma$  represents the effect of super-zone boundary, which causes a rapid increase of resistivity just below  $T_N$ . Similarly to Eq. (1), the magnetoresistance due to these AFM correlations can be expressed as

$$\text{MR} \propto \frac{m_Q(H, T)^2 - m_Q(0, T)^2}{1 - \Gamma m_Q(0, T)} \propto m_Q(H, T)^2 - m_Q(0, T)^2. \quad (2)$$

Hence, both Eqs. (1) and (2) give  $\text{MR} \propto m(H, T)^2 - m(0, T)^2$  except the difference in the denominator. Following the discussion of Fig. 1, a similar effect should be expected for Ni-Mn-Sn films below MT since in off-stoichiometric Ni-Mn-X HA, the martensitic transformation is the first-order transformation accompanied with an increase of AFM correlations.<sup>5,13,14</sup> We assume that the increase in resistivity of Ni-Mn-Sn film at MT is due to the presence of incipient AFM coupling between Mn atoms which strengthens below MT.<sup>5</sup> Our exemplary data of MR( $H$ ) [Fig. 3(a)] are consistently presented in Fig. 5 within the framework of the phenomenological model. It can be seen that MR varies linearly as a function of  $M(H, T)^2 - M_S^2$  regardless MR is measured in AP or MP. In the vicinity of MT (110 K), MR varies nonlinearly due to

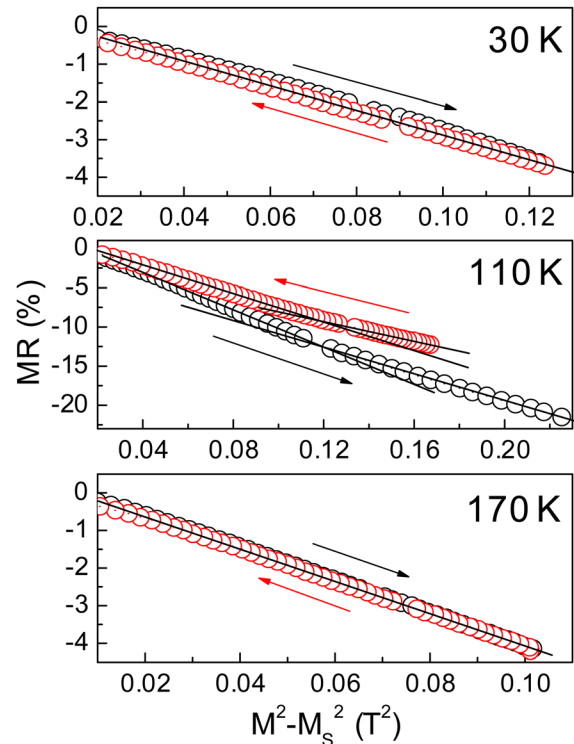


FIG. 5. MR in Ni-Mn-Sn epitaxial film as a function of  $M(H, T)^2 - M_S^2$  in MP (30 K), in MT region (110 K) and in AP (170 K). Data points depicted with light and black open circles represent MR measured in the first and the second field cycle, respectively. Straight lines serve as guides for eye.



metamagnetic-like behavior on increasing the field [cycle 1 in Fig. 3(b)] and kinetic arrest [see, cycle 2 in Fig. 3(b)]. Nevertheless, the nonlinear behavior of MR at 110 K may be reasonably linearized in two field ranges as shown in Fig. 5 in agreement with the relations (1) and (2).

In conclusion, magnetotransport of Ni<sub>50</sub>Mn<sub>35</sub>Sn<sub>15</sub> epitaxial films has been studied as a function of temperature and magnetic field. The MR is consistently analyzed both in the framework of frequently applied functional relationship<sup>3</sup> and phenomenological model originated from microscopic spin disorder theory.<sup>8</sup> It is found that MR scales as the square of magnetization  $\Delta m(H, T)^2$ . Since  $\Delta m(H, T)$  at MT is the highest for Ni-Mn-In alloys,<sup>5,6</sup> one should expect that MR is the highest, too, as it has been confirmed experimentally.<sup>6</sup> On the other hand, only a modest MR occurs in Ni-Mn-Ga with no AFM correlations because  $\Delta m(H, T)$  is only of a few percent.<sup>7</sup>

This work was partially supported by the Polish Ministry of Science and Higher Education Grant No. 733/N-DAAD/2010/0.

<sup>1</sup>A. N. Vasilev, A. D. Bozhko, V. V. Khovailo, I. E. Dikstein, V. G. Shavrov, V. D. Buchelnikov, M. Matusmoto, T. Takagi, and J. Tani, *Phys. Rev. B* **59**, 1113 (1999).

<sup>2</sup>T. Krenke, M. Acet, E. F. Wassermann, X. Moya, L. Mañosa, and A. Planes, *Phys. Rev. B* **72**, 014412 (2005); T. Krenke, E. Duman, M. Acet, E. F. Wassermann, X. Moya, L. Mañosa, and A. Planes, *Nature Mater.* **4**, 450 (2005).

<sup>3</sup>S. Singh and C. Biswas, *Appl. Phys. Lett.* **98**, 212101 (2011).

<sup>4</sup>K. Koyama, H. Okada, K. Watanabe, T. Kanomata, R. Kainuma, K. Oikawa, W. Ito, and K. Ishida, *Appl. Phys. Lett.* **89**, 182510 (2006).

<sup>5</sup>A. Planes, L. Mañosa, and M. Acet, *J. Phys.: Condens. Matter* **21**, 233201 (2009), and references therein.

<sup>6</sup>V. K. Sharma, M. K. Chattopadhyay, K. H. B. Shaeb, A. Chouhan, and S. B. Roy, *Appl. Phys. Lett.* **89**, 222509 (2006).

<sup>7</sup>J. M. Barandiarán, V. A. Chernenko, P. Lázpita, J. Gutiérrez, and J. Feuchtwanger, *Phys. Rev. B* **80**, 104404 (2009).

<sup>8</sup>T. Kasuya, *Prog. Theor. Phys.* **16**, 58 (1956); P. G. de Gennes and J. Friedel, *J. Phys. Chem. Solids* **4**, 71 (1958); T. van Peski-Tinbergen and A. J. Dekker, *Physica* **29**, 917 (1963); M. Kataoka, *Phys. Rev. B* **63**, 134435 (2001).

<sup>9</sup>R. J. Elliot, in *Theory of Magnetism in the Rare Earth Metals*, Magnetism Vol. **IIA**, edited by G. T. Rado and H. Suhl (Academic, New York, 1965).

<sup>10</sup>J. Dubowik, I. Gościańska, K. Załęski, H. Głowiński, A. Ehresmann, G. Kakazei, and S. A. Bunayev, "Epitaxial growths and magnetization dynamics of Ni<sub>2</sub>MnSn Heusler alloy films," *Acta Phys. Pol. A* (unpublished).

<sup>11</sup>V. D. Buchelnikov, V. V. Khovailo, and T. Takagi, *J. Magn. Magn. Mater.* **300**, e459 (2006).

<sup>12</sup>A. L. Roytburd, T. S. Kim, Q. Su, J. Slusker, and M. Wuttig, *Acta Mater.* **46**, 5095 (1998).

<sup>13</sup>S. Chattarjee, S. Giri, S. Majumdar, and S. K. De, *J. Phys. D: Appl. Phys.* **42**, 065001 (2005).

<sup>14</sup>S. Aksoy, M. Acet, P. P. Deen, L. Mañosa, and A. Planes, *Phys. Rev. B* **79**, 212401 (2009).

<sup>15</sup>V. Kumar, S. Chattarjee, and R. C. O' Handly, *Appl. Phys. Lett.* **89**, 222107 (2006).

<sup>16</sup>V. V. Khovailo, V. Novosad, and T. Takagi, *Phys. Rev. B* **70**, 174413 (2004).

<sup>17</sup>M. Kohl, D. Dittmann, E. Quandt, and B. Winzek, *Sens. Actuators* **83**, 214 (2000).

<sup>18</sup>S. Banik, R. Rawat, P. K. Mukhopadhyay, B. L. Ahuja, A. Chakrabarti, P. L. Paulose, S. Singh, A. K. Singh, D. Pandey, and S. R. Barman, *Phys. Rev. B* **77**, 224417 (2008).

<sup>19</sup>S. Yuasa, T. Akiyama, H. Miyajima, and Y. Otani, *J. Phys. Soc. Jpn.* **64**, 3978 (1995).